Climate
of the Past

Particle shape accounts for instrumental discrepancy in ice core dust size distributions

Marius Folden Simonsen[1], **Llorenç Cremonesi**[2], **Giovanni Baccolo**[4], **Samuel Bosch**[1], **Barbara Delmonte**[4], **Tobias Erhardt**[3], **Helle Astrid Kjær**[1], **Marco Potenza**[2], **Anders Svensson**[1], and **Paul Vallelonga**[1]

[1]Centre for Ice and Climate, Niels Bohr Institute, University of Copenhagen, Copenhagen, Denmark
[2]Department of Physics, University of Milan and National Institute for Nuclear Physics (INFN),
Via Celoria 16, I20133 Milan, Italy
[3]Climate and Environmental Physics, Physics Institute & Oeschger Centre for Climate Change Research,
University of Bern, Sidlerstrasse 5, 3012 Bern, Switzerland
[4]Department of Earth and Environmental Sciences, University Milano-Bicocca, Piazza della Scienza 1,
I20126 Milan, Italy

Correspondence: Marius Folden Simonsen (msimonse@fys.ku.dk)

Abstract. The Klotz Abakus laser sensor and the Coulter counter are both used for measuring the size distribution of insoluble mineral dust particles in ice cores. While the Coulter counter measures particle volume accurately, the equivalent Abakus instrument measurement deviates substantially from the Coulter counter. We show that the difference between the Abakus and the Coulter counter measurements is mainly caused by the irregular shape of dust particles in ice core samples. The irregular shape means that a new calibration routine based on standard spheres is necessary for obtaining fully comparable data. This new calibration routine gives an increased accuracy to Abakus measurements, which may improve future ice core record intercomparisons. We derived an analytical model for extracting the aspect ratio of dust particles from the difference between Abakus and Coulter counter data. For verification, we measured the aspect ratio of the same samples directly using a single-particle extinction and scattering instrument. The results demonstrate that the model is accurate enough to discern between samples of aspect ratio 0.3 and 0.4 using only the comparison of Abakus and Coulter counter data.

1 Introduction

Ice cores from Greenland contain a record of climate proxies over the last 120 000 years. One of those proxies is mineral dust in the size range 0.5–100 µm. The dust has several properties that provide useful information of the past: concentration, size distribution, morphology and chemical and isotopic composition. These measurements have revealed that the dust in ice cores come from central Asia during both the Holocene and the last glacial period (Biscaye et al., 1997). The observed 100-fold decrease in dust concentration from glacial to Holocene (Ruth et al., 2003; Steffensen, 1997) has constrained the aridity, windiness and insolation forcing of glacial climate models (Mahowald et al., 1999; Lambert et al., 2015).

Traditionally, the Coulter counter technique has been used to measure concentration and size distribution. It works by measuring the electrical impedance over an orifice through which a sample flows. For ice cores, this sample is melted ice core water, with pure NaCl added to stabilize the electrical conductivity. When a particle flows through and displaces the conductive liquid, the impedance rises. This signal increases with the particle volume. The Coulter counter has the disadvantage that it applies only to discrete samples and has not been combined with continuous flow analysis (CFA) systems.

CFA systems (Röthlisberger et al., 2000; Kaufmann et al., 2008), on the other hand, are a common technique for analyzing impurities in ice core samples, offering a faster measurement speed and often higher resolution. On the Copenhagen CFA system, $35 \times 35 \times 550$ mm sticks are cut from the ice core and melted upon a gold-coated melt head (Bigler et al., 2011). The meltwater from the outer 5 mm of the ice core surface is discarded, while the inner uncontaminated water is transported by a peristaltic pump to the connected instruments. One of these instruments is the Abakus laser sensor (LDS23/25bs; Klotz GmbH, Germany) for measuring insoluble particle concentration and size distribution.

The Abakus instrument measures the intensity of laser light through a flow cell filled with the sample liquid. When a particle passes, the light is attenuated. The Abakus therefore measures the optical extinction cross section of the particle and can measure particles in the range 1–15 µm. Since it measures optical transmissivity rather than electrical impedance, it is much less sensitive to electrical noise than the Coulter counter. The Abakus on a CFA system can have a measurement depth resolution of 3 mm (Bigler et al., 2011) and requires almost no maintenance when the CFA system is running. The Coulter counter, on the other hand, typically integrates a thicker depth interval and requires work from the operator at all times during measurements (Delmonte et al., 2004; Lambert et al., 2012).

The aspect ratio of ice core dust particles was measured using the novel single-particle extinction and scattering (SPES) instrument (Villa et al., 2016; Potenza et al., 2016). The SPES measures both the extinction cross section, which is also measured by the Abakus, and the optical thickness of the particles (Potenza et al., 2016).

The optical thickness depends on the geometrical thickness of the particle and its refractive index. If the refractive index is known, the aspect ratio can be derived from the combination of extinction cross section and geometrical thickness. The SPES is able to discern between oblate and prolate particles.

The extinction and scattering cross sections of irregularly shaped particles can be accurately calculated with the discrete dipole approximation (DDA) (Draine and Flatau, 1994). In the present work, we have used the Amsterdam Discrete Dipole Approximation (ADDA) code (Yurkin and Hoekstra, 2011). The ADDA simulations were used to simulate the SPES measurements and thereby extract the aspect ratio from the SPES data. Furthermore, the ADDA simulations were used to show that the Mie scattering effects on the optical extinction cross section for spherical particles do not affect ice core dust due to its irregular shape (Chylek and Klett, 1991).

The measured samples are from the Renland Ice Cap Project (RECAP) ice core drilled during the summer of 2015 on the Renland ice cap in eastern Greenland only 2 km away from the old Renland ice core (Hansson, 1994). This ice core covers the last glacial cycle, and samples were taken from
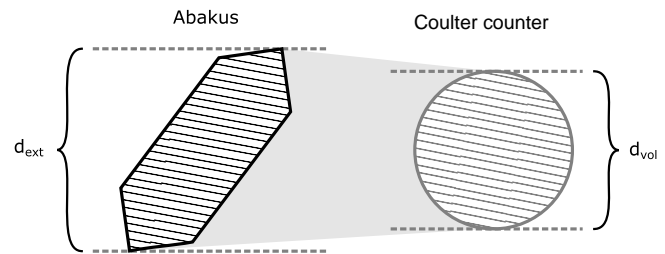

Figure 1. The Abakus measures the extinction cross section of the particles, while the Coulter counter measures their volume. Both instruments convert this to an equivalent diameter, d_{ext} and d_{vol}, respectively.

both the Holocene and the last glacial period (the Supplement A). As found for the central Greenlandic ice cores, the glacial RECAP dust comes from central Asia (Biscaye et al., 1997). The Holocene dust, similar to the old Renland core (Bory et al., 2003), is dominated by a local East Greenlandic source. The volume mode of the glacial dust is 2 µm, versus 20 µm for the Holocene dust, due to the increased transport size fractionation for the glacial dust (Ruth et al., 2003).

Although both instruments are typically calibrated using standard spheres of known diameter, they produce substantially different size distribution results when ice core samples are measured (Ruth et al., 2003; Lambert et al., 2008, 2012; Koffman et al., 2014). It has been proposed that this difference is because ice core dust is generally nonspherical (Lambert et al., 2012; Potenza et al., 2016). We show here that the nonspherical shape of the particles does quantitatively account for the main discrepancy between the two instruments (Fig. 1). One important shape effect arises from the aspect ratio, defined as the ratio between the length of its shortest and longest side. We have found that Greenland ice core dust is dominated by oblate particles of aspect ratio 0.3–0.4, which is significantly different from the aspect ratio of 1 of the polystyrene standard spheres used for calibration.

2 Materials and methods

2.1 Abakus

For the Abakus measurements, square sticks of $35 \times 35 \times 550$ mm were cut from the center of the RECAP ice core. These sticks were melted on the RECAP CFA system. This CFA system is an enlargement of the one described by Bigler et al. (2011), with a higher melt rate, more analytical channels and pressure decoupling after the debubbler. The Abakus was connected to the CFA system with a flow rate of 2 mL min^{-1}. The attached tubes and the Abakus were cleaned with MQ water (Millipore Advantage, 18.2 MOhm cm^{-1}) after each 5.5 m of ice measured. Occasionally the Abakus was clogged by a large particle and required flushing with a syringe while the system was running. The depth resolution is 5 mm due to mixing in the tubes from

the melt head to the Abakus. For high dust concentrations, two particles may pass through the detector at the same time and show up as one larger particle. We found that this effect was negligible (see the Supplement B for details). The Abakus was originally calibrated to give the correct diameter for polystyrene beads of 2, 5 and 10 µm.

Polystyrene standard spheres of 1.5, 2, 4, 5 and 10 µm in diameter from BS-Partikel GmbH, Wiesbaden, Germany (the Supplement C) were measured by the Abakus. They were diluted to concentrations between 15 000 and 90 000 particles mL^{-1}. To avoid coagulation, the standards were sonicated for 30 s before measurements. Each of the standards was measured for 6 min.

2.2 Coulter counter

The Coulter counter measured discrete samples 55 cm in length. The measured ice consisted of an outer triangular piece 3×1 cm in cross section cut to 10 cm long pieces. The samples were decontaminated by rinsing in three consecutive jars of MQ water. In each jar the outer layer of ice was melted away and removed, leaving only the cleaner inner part to be analyzed. This treatment reduced the sample size by 50 %. The samples were measured in two Beckman Coulter counters, one with a 100 µm aperture and one with a 30 µm aperture. The samples were shaken prior to measurement in the 100 µm Coulter counter. Afterwards the samples were measured by the 30 µm Coulter counter. The 30 µm aperture data were used for particles smaller than 4 µm and the 100 µm aperture data were used for particles larger than 4 µm. Selected samples representative of Holocene and glacial climates were measured by the Coulter counter for this study. For the Holocene, selected samples from 356 to 4008 years b2k (before AD 2000) were used, while for the glacial, the whole period from 17 760 to 33 885 years b2k was measured (the Supplement A). The same samples were used for the Abakus.

2.3 SPES

After the Coulter counter measurements, the samples were measured by SPES (Sect. 3.3). The sample flows through a 200 µm flow cell and is illuminated by a laser. The light is measured by two detectors, which in combination give the extinction cross section and the optical thickness. There is no focusing of the particle stream in the cell, so only a small fraction of the particles passing through the cell is measured by the laser. Therefore the sample is circulated through the cell several hundred to thousand times. This gives an accurate measure of the shape distribution of the particles, but it does not allow for concentration measurements.

The narrow cell ensures high shear, forcing the particles to attain a preferential direction. Oblate particles in a shear flow orient themselves with the flat side along the flow lines and are randomly oriented in the shear direction. Prolates lie in a plane of constant velocity and are free to rotate within it (Jeffery, 1922).

3 Results

3.1 ADDA simulations

Using the Amsterdam Discrete Dipole Approximation software (ADDA) (Yurkin and Hoekstra, 2011), we have calculated the extinction diameter for different particles. The extinction diameter is based on the optical extinction cross section. The optical extinction cross section is defined for a plane light wave interacting with a particle as the difference between the incoming and transmitted light intensity divided by the incoming light intensity and multiplied by the area of the plane incoming wave. For spherical particles much larger than the wavelength of the light, the relation between diameter and optical extinction cross section is $\sigma_{\text{ext}} = \frac{\pi}{2}d^2$. For smaller particles of a size comparable to the light wavelength, the relation differs due to optical effects (Fig. 2) (van de Hulst, 1957). However, we define the extinction diameter as $d_{\text{ext}} = \sqrt{\frac{2}{\pi}\sigma_{\text{ext}}}$ for all particles. We associate each particle with its volumetric diameter: a sphere with volume V has the diameter $d_{\text{vol}} = \sqrt{[3]\frac{6V}{\pi}}$. For any particle of known volume, the volumetric diameter is given by this relation.

Specifically, we have used ellipsoids and oblate prisms with an aspect ratio of 0.3 in the volumetric diameter range 1 to 8 µm (Fig. 3). While spheres have a unique extinction diameter for each volumetric diameter, the extinction diameter of other particles depends on their orientation. For each volumetric diameter, there will therefore be several possible Abakus measurements of the extinction diameter described by a probability density function. This is described in more detail in Sect. 3.4, where it is called $\frac{\text{d}P(d_{\text{ext}}|d_{\text{vol}})}{\text{d}\ln d_{\text{ext}}}$. The broadness of the probability density function for nonspherical particles results in a smoothing of the relationship between the extinction and volumetric diameters (Fig. 3). Furthermore, the extinction diameter oscillation maxima are not located at the same d_{vol} for different particle shapes. Since ice core dust has a variable shape (the Supplement D), it is sampled from a sum of the ellipsoid, prismatic and many more distributions. In this sum of distributions the oscillation pattern averages out.

The average extinction diameter is larger than the volumetric diameter since the measured dust particles are elongated (discussed further in Sect. 3.4). For particles larger than 1.7 µm, the average extinction diameter is approximately proportional to the volumetric diameter. For much smaller particles, the extinction diameter is independent of the particle shape. After calibration, the Abakus cannot measure particles with an extinction diameter smaller than 1.8 µm, so the measured Abakus data are within the range of proportionality: $d_{\text{ext}} \propto d_{\text{vol}}$ (Sect. 3.2).
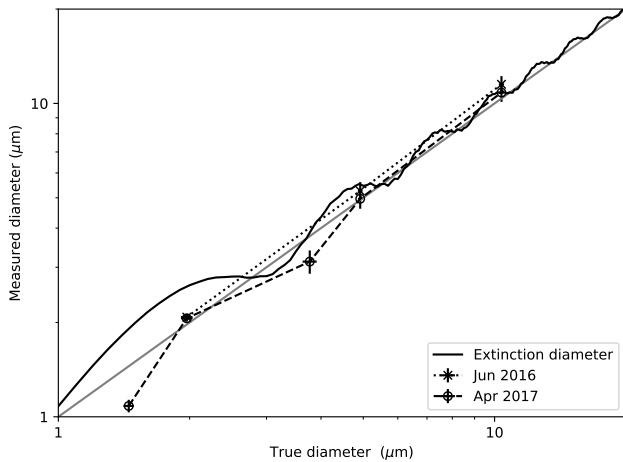
Figure 2. The diameter of standard polystyrene spheres measured by the Abakus as a function of the true diameter certified by the manufacturer (circles and dashed line), together with three of the same standards measured a year earlier (crosses and dotted line) and the optical extinction diameter of a sphere as a function of diameter (solid black curve). The grey line is where the measured and the true diameter are equal, to which the extinction diameter converges for large true diameters.
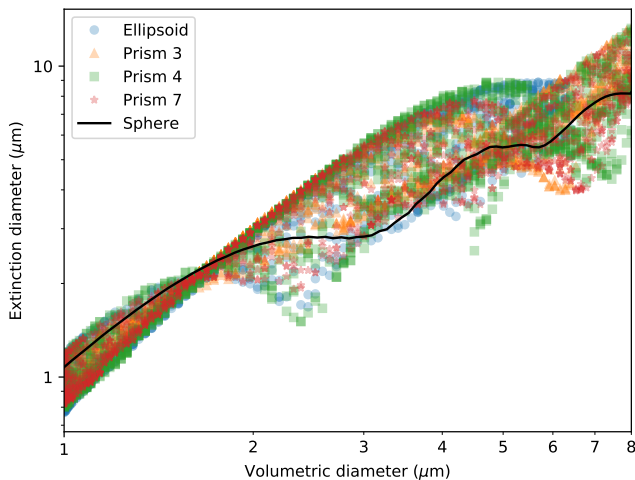

Figure 3. ADDA simulations of particles with a refractive index of 1.586 and, except for the spheres, an aspect ratio of 0.3. The prisms are oblate and their cross sections are equilateral polygons with 3, 4 and 7 sides.

3.2　Extinction calibration using particle size standards

We have measured the diameters of five different particle size standards (the Supplement C, Sect. 2.1) with the Abakus (Fig. 2). The 2, 5 and 10 μm standards were measured twice with a 1-year delay, without significantly different results. This shows that the Abakus calibration is stable over the timescale of a typical measurement campaign.

Since d_{ext} is proportional to d_{vol} for ice core dust (Sect. 3.1) and the proportionality constant depends on particle shape and is unknown, we would like to calibrate the Abakus such that it gives the extinction diameter d_{ext} and not the true diameter for the standard spheres (using the term true for the certified diameter given by the manufacturer). Therefore we define a calibration function such that the measured diameter divided by the calibration function is the extinction diameter. To avoid artifacts in the calibrated distribution, the calibration function has to be a continuous function of the measured diameter with a continuous first derivative. Since we want the relative error in each standard to have the same weight, the function is fitted to the logarithm of the ratio between the measured and extinction diameter. The function $y = a(x - x_0)^2$, where $y = \frac{\ln(d_{meas})}{\ln(d_{ext})}$ and $x = \ln(d_{meas})$, is fitted to the data as a calibration function (Fig. 4). The fit parameters found are $(a, x_0) = (-0.086, 2.60)$. This particular calibration function is chosen because it is simple, fits the data well and satisfies the conditions described above. $x_0 = 2.60$ corresponds to $d_{meas} = 13.5$ μm. As the calibration function is equal to 1 for $d_{meas} = 13.5$ μm and standards larger than 13.5 μm were not tested, no calibration is applied for diameters larger than 13.5 μm.

The particle size standard calibration has been applied to ice core dust data (orange curves in Fig. 5a, b). Since the calibration function is less than 1 for diameters smaller than 13.5 μm, the effect of applying the calibration function is that the small diameter data are shifted towards larger diameters. This is most pronounced for the smallest diameters, since the calibration values are smallest for small diameters. The positive slope of the calibration function means that the calibrated bin positions are squeezed more tightly together than the uncalibrated bins. Since the probability density function is defined as the number of counts in a bin divided by its size, the calibrated probability density function has higher values than the uncalibrated one. This effect decreases with diameter as the slope decreases. For further details, see the Supplement E.

3.3　SPES

We have measured optical thickness (ρ) and extinction cross section (σ_{ext}) with SPES for both Holocene and glacial samples (Fig. 6) using the method of Villa et al. (2016) and compared the results to ADDA simulations. The distribution of particles in ρ, σ_{ext} space can be simulated using ADDA for a given particle shape and size distribution. We have done this for oblate right square prisms of aspect ratios 0.2, 0.25, 0.3, 0.4 and 0.5. A total of 20 000 particles with a volumetric diameter ranging from 100 nm to 2 μm and different refractive indices and orientations were simulated. This size range covers the SPES measurement range.

The refractive index, n, of atmospheric dust is on average between 1.52 and 1.55 (Shettle and Fenn, 1979; Sokolik et al., 1993; Grams et al., 1974). At Dome C in Antarctica,
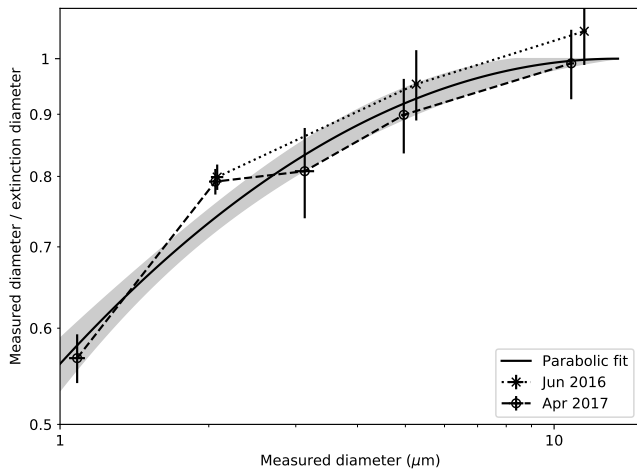
Figure 4. The ratio between the diameter of spheres measured by the Abakus in April 2017 and their extinction diameter (Fig. 2) (circles and dashed line), together with three of the same standards measured a year earlier (crosses and dotted line) and a fit to the logarithm of the April 2017 data (solid line). The fitted parameters are $(a, x_0) = (-0.086, 2.60)$ of the function $a(x - x_0)^2$, where x is the logarithm of the diameter in μm. The uncertainty on the fit (shading) is based on the uncertainty in the data points.

Figure 5. Size distributions of the dust particles in the RECAP ice core for both the Holocene and last glacial period measured by the Abakus and Coulter counter. **(a, b)** Probability density functions of the number of particles as a function of volumetric diameter, measured diameter or extinction diameter for Coulter counter (black, volumetric diameter), raw Abakus (blue, measured diameter), extinction calibrated Abakus (Sect. 3.2) (orange, extinction diameter), modeled Abakus data based on Coulter counter data and the aspect ratio measured by SPES (Sect. 3.4) (green, extinction diameter), and Abakus data fully calibrated to Coulter counter data using both the extinction calibration and aspect ratio (Sect. 3.5) (red, volumetric diameter). The uncertainty (shaded area) in the raw Abakus data is measurement uncertainty (the Supplement H), while the remaining uncertainties are linearly propagated from the Abakus and aspect ratio uncertainties. **(c, d)** Raw Abakus data divided by Coulter counter (blue, from blue and black in **a, b**), extinction calibrated Abakus data divided by modeled Abakus data (orange, from orange and green in **a, b**) and fully calibrated Abakus data divided by Coulter counter (red, from red and black in **a, b**). **(e, f)** Probability density functions of particle volume derived from the number density functions in **(a, b)** for Coulter counter (black), raw Abakus (blue) and fully calibrated Abakus data (red).

the refractive index of Holocene and glacial ice core dust is 1.53 and 1.56 (Royer et al., 1983). We have run the simulations using the refractive indices 1.52 and 1.55 and found only a small effect of the refractive index on the modeled aspect ratio.

By comparing to SPES measurements of oblate and prolate particles in Villa et al. (2016) and Potenza et al. (2016), it was found that the samples are dominated by oblates. Prolates have a much narrower distribution of optical thickness than oblates, since their orientation is fixed by the flow. The absence of a superimposed prolate distribution indicates that no more than 15 % of the particles are prolates. The following analysis therefore only focuses on oblates. For a similar analysis of prolates, see the Supplement F.

To compare the simulations and the data, the average of the logarithm of the simulated optical thickness as a function of extinction cross section was calculated. This average was then used as a least squares fit to the measured data, for which the aspect ratio is the variable parameter. For values of σ_{ext} approaching the lower and upper bound of the extinction cross section range, the SPES is not sensitive in the full optical thickness range. To avoid bias, only experimental data between the 0.25 and 0.75 quantile of the extinction cross section were used in the fit.

For $n = 1.52$ the Holocene aspect ratio is 0.42 ± 0.03 and the glacial is 0.38 ± 0.02, while for $n = 1.55$ the Holocene is 0.36 ± 0.01 and the glacial is 0.29 ± 0.01. This is independent of the volumetric diameter size distribution used in the simulation. The average in the refractive index range of ice core
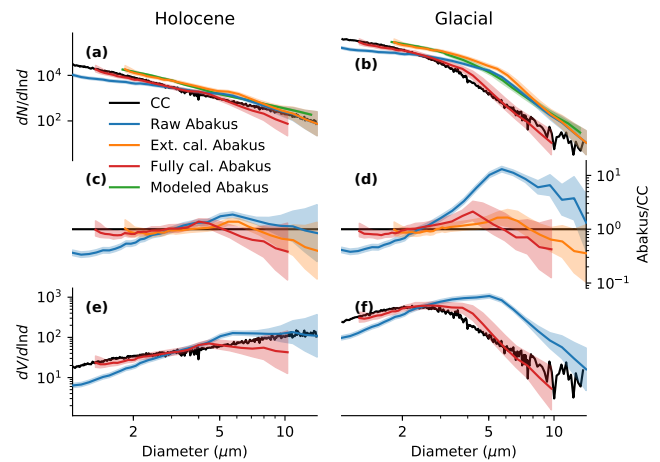
dust is therefore 0.39 ± 0.03 for the Holocene and 0.33 ± 0.04 for the glacial.

3.4 Aspect ratio effect

Spheres have the lowest geometrical cross section to volume of all particles when averaged over all rotation angles of the particles (Brazitikos et al., 2014). We define the geometric cross section diameter of a particle as $d_{\text{geom}} = \sqrt{\frac{2}{\pi} \sigma_{\text{geom}}}$, where σ_{geom} is the geometric cross section of the particle. However, since ice core dust is nonspherical (Sect. 3.3), $d_{\text{geom}} > d_{\text{vol}}$ and $d_{\text{ext}} = d_{\text{geom}}$ (Sect. 3.2). We can therefore calculate the distribution of d_{ext} based on the aspect ratio c and the distribution of d_{vol}. The distribution of d_{vol}, $\frac{dP(d_{\text{vol}})}{d\ln d_{\text{vol}}}$, can be determined by the Coulter counter.

Since oblates dominate the measured samples, we will focus our model on those instead of also considering prolates
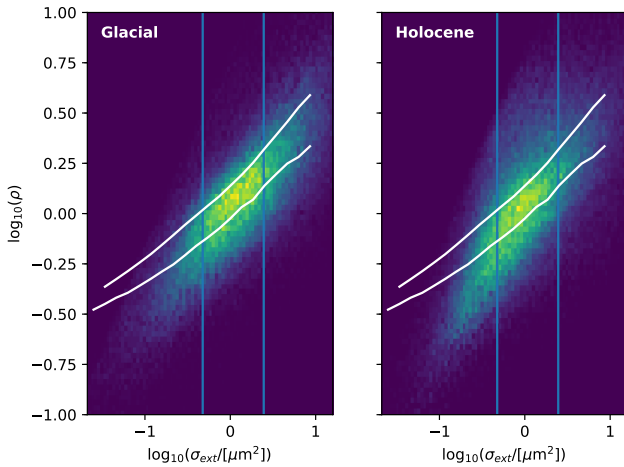
Figure 6. Glacial and Holocene samples measured by SPES. The brighter colors have a higher number of measured particles in a bin. The blue lines mark the 0.25 and 0.75 quantiles of σ_{ext}. The white curves are the mean optical thickness as a function of σ_{ext} for ADDA simulations with a refractive index of 1.55. The upper is for an aspect ratio of 0.5, the lower for 0.2.

(Sect. 3.3). As previously mentioned (Sect. 2.3), oblate particles in a shear flow orient themselves with the flat side along the flow lines, while they are randomly oriented in the shear direction (Jeffery, 1922). Since they are free to rotate along an axis orthogonal to the light beam direction, we can model them as rectangles embedded in two dimensions for which all orientation angles are equally likely (the Supplement G). The light and detector also lie in the plane. In this 2-D model, d_{vol} is the square root of the area of the rectangle, and d_{ext} is the cross section of the rectangle.

Denoting the length of the short side b, the length the long side a and the aspect ratio $c = b/a$, the probability of d_{ext} given a certain d_{vol} is

$$\frac{dP(d_{\text{ext}}|d_{\text{vol}})}{d\ln d_{\text{ext}}} = \begin{cases} 0 & \text{for } d_{\text{ext}} < b \\ z & \text{for } b < d_{\text{ext}} < a \\ 2z & \text{for } a < d_{\text{ext}} < \sqrt{a^2 + b^2} \end{cases}, \quad (1)$$

for

$$z = \frac{2}{\pi} \frac{1}{\sqrt{\frac{a^2 + b^2}{d_{\text{ext}}^2} - 1}}. \quad (2)$$

The distribution of d_{ext} for all d_{vol} can then be found as

$$\frac{dP(d_{\text{ext}})}{d\ln d_{\text{ext}}} = \int \frac{dP(d_{\text{ext}}|d_{\text{vol}})}{d\ln d_{\text{ext}}} \frac{dP(d_{\text{vol}})}{d\ln d_{\text{vol}}} d\ln d_{\text{vol}}. \quad (3)$$

In Sect. 3.2 we calibrated the Abakus such that $d_{\text{meas}} = d_{\text{ext}}$. Therefore $\frac{dP(d_{\text{ext}})}{d\ln d_{\text{ext}}}$ calculated here simulates Abakus measurements.

This can be used to find the aspect ratio of the particles just from the Coulter counter–Abakus discrepancy. To do this, the sum of the square of the logarithm of the ratio between $\frac{dP(d_{\text{ext}})}{d\ln d_{\text{ext}}}$ as calculated from the Coulter counter data and the Abakus data was minimized with respect to the aspect ratio. This gives the aspect ratio in which $\frac{dP(d_{\text{ext}})}{d\ln d_{\text{ext}}}$ is most consistent with the Abakus data, which is the most likely aspect ratio given the data. For the Holocene data this gave $c = 0.41 \pm 0.09$, while for the glacial $c = 0.31 \pm 0.04$. The errors are propagated from the total errors on the calibrated Abakus data. There is, however, a large correlation between the errors in the Holocene and glacial data, so the error in the difference is only around 0.02, confirming a significant difference in aspect ratio between glacial and Holocene dust particles.

3.5 Calibration of Abakus

Equation (3) gives the extinction diameter size distribution (Abakus) given a measured volumetric size distribution (Coulter counter) and a known aspect ratio. However, often a measurement of the volumetric size distribution is desired, while only Abakus measurements are available. This requires the inversion of Eq. (3), which cannot be done analytically. However, multiplying the extinction calibrated Abakus bins by the cubic root of the aspect ratio is a good approximation. This gives the fully calibrated Abakus data of Fig. 5. For the glacial volumetric distributions, the modes of the Coulter counter, the uncalibrated Abakus and the fully calibrated Abakus data are 2.3, 5.0 and 2.7 µm, respectively. Further details on the calibration are found in the Supplement E.

4 Discussion

Ruth et al. (2008, Fig. 1a) demonstrated that the data produced by the Coulter counter and Abakus are proportional over 4 orders of magnitude, even if the absolute concentration results do not agree. This is partly because the instruments have different detection limits (see the Supplement I) and partly because they measure two different properties of the particles: volumetric and extinction cross section. When the Abakus is calibrated using the true diameter of polystyrene spheres, it gives up to 10 times as many counts as the Coulter counter for some particle sizes when ice core samples are measured (Fig. 5). It is not possible in general to calibrate the Abakus such that it yields the same distribution as the Coulter counter for all ice core samples. However, by combining Coulter counter and Abakus data, additional information is gained about the aspect ratio that was not available from the two instruments individually.

It has previously been suggested that it is impossible to calibrate the Abakus using polystyrene beads due to the strong Mie oscillations (Ruth, 2002, p. 20). It was argued that since for spheres the measured extinction cross section is a non-monotonous function of the true diameter, it can-

not be inverted. However, this is based on the criterion that d_{meas} of the Abakus should be identical to d_{true} when measuring spheres. Since spheres have strong Mie oscillations but ice core dust does not, this criterion is invalid. Therefore the Abakus should be calibrated such that d_{meas} is equal to d_{ext} instead of d_{true} (Sect. 3.2).

With the SPES instrument we found that the average aspect ratio of our ice core dust samples is 0.39 ± 0.03 for the Holocene and 0.33 ± 0.04 for the glacial, so the particles are significantly elongated (Sect. 3.3). Using our simple model for the relation between d_{meas} and d_{vol}, we have calculated the aspect ratio independently from the Abakus and Coulter counter data. This gave an aspect ratio of 0.41 ± 0.09 for the Holocene and 0.31 ± 0.04 for the glacial in accordance with SPES. The SPES aspect ratio was calculated for particles less than $2\,\mu\text{m}$ in volumetric diameter and the Abakus for particles between 1.2 and $9\,\mu\text{m}$, so the measurements are not directly comparable. However, as we only investigate the leading order effect of the aspect ratio and atmospheric studies find no size dependence of the aspect ratio (Knippertz and Stuut, 2014, p. 28), it is assumed that any possible size dependence of the aspect ratio is not large enough to significantly change the results. In addition to giving the same aspect ratio as SPES, the model also gives a consistent size distribution within the Abakus uncertainties (Fig. 5).

In the Dome C ice core from the East Antarctic plateau the aspect ratios of oblate and prolate particles have been determined to be 0.2 ± 0.1 and 3.5 ± 1.3, respectively (Potenza et al., 2016). The ranges refer to the variability in the aspect ratio among different particles and not the uncertainty of the mean. In the RECAP ice core studied here, we found a similar but slightly less extreme aspect ratio in both the Holocene and the glacial ice. For the RECAP core, we speculate that the Holocene dust originates from local eastern Greenlandic sources, while the glacial dust is from central Asia (Bory et al., 2003). Measurements of dust particles in dust storms generally show an aspect ratio above 0.5. However, during transport, the dust fractionates towards more extreme aspect ratios (Knippertz and Stuut, 2014, pp. 28–30). Since large ice sheets are located far from typical dust sources, the dust extracted from ice cores would be subject to more fractionation. Therefore we do expect more extreme aspect ratios to be found in ice core dust than in the atmospheric dust storm measurements. The greater aspect ratio of the local Greenlandic Holocene dust compared to the Asian glacial dust agrees well with the aspect ratio fractionation observed in the atmosphere.

5   Conclusions

The Abakus laser sensor and the Coulter counter give different size distributions when measuring the same ice core dust sample. This is because ice core dust particles are not spherical, so the particle volume measurements of the Coul-

ter counter are different from the cross section measurements of the Abakus. When spherical particles are measured by the Abakus, the measured extinction diameter oscillates strongly as a function of particle size due to Mie scattering oscillations. The extinction diameter of ice core dust does not show this oscillation pattern, but is proportional to the volumetric diameter. When the Abakus is calibrated using spherical particles, it should therefore be calibrated to the extinction diameter and not to the true diameter.

We derived a model for extracting the aspect ratio of the dust particles from the differences between Abakus and Coulter counter measurements of the same ice core dust samples. This process suggests an aspect ratio of 0.41 ± 0.01 for Holocene and 0.32 ± 0.01 for glacial dust samples from the RECAP ice core, which is consistent with direct aspect ratio measurements from a single-particle extinction and scattering instrument. This shows that not only is the discrepancy between the two instruments explained by the nonspherical shape of the particles, but it can also be used to obtain the aspect ratio. As the Holocene dust has Greenlandic origin, while the glacial dust is Asian, the aspect ratio could potentially aid in provenance determination and in understanding atmospheric transport processes. Moreover, by determining the aspect ratio, a better size distribution can be obtained from the Abakus data.

The Supplement related to this article is available online at https://doi.org/10.5194/cp-14-601-2018-supplement.

References

Bigler, M., Svensson, A., Kettner, E., Vallelonga, P., Nielsen, M. E., and Steffensen, J. P.: Optimization of high-resolution continuous

flow analysis for transient climate signals in ice cores, Environ. Sci. Technol., 45, 4483–4489, 2011.

Biscaye, P., Grousset, F., Revel, M., Van der Gaast, S., Zielinski, G., Vaars, A., and Kukla, G.: Asian provenance of glacial dust (stage 2) in the Greenland Ice Sheet Project 2 ice core, Summit, Greenland, J. Geophys. Res.-Ocean., 102, 26765–26781, 1997.

Bory, A. J.-M., Biscaye, P. E., Piotrowski, A. M., and Steffensen, J. P.: Regional variability of ice core dust composition and provenance in Greenland, Geochem. Geophy. Geosy., 4, 1107, https://doi.org/10.1029/2003GC000627, 2003.

Brazitikos, S., Giannopoulos, A., Valettas, P., and Vritsiou, B.: Geometry of Isotropic Convex Bodies: Mathematical Surveys and Monographs, Am. Math. Soc., 2014.

Centre for Ice and Climate: Data, icesamples and software, www.iceandclimate.dk/data, 2018.

Chylek, P. and Klett, J. D.: Extinction cross sections of nonspherical particles in the anomalous diffraction approximation, JOSA A, 8, 274–281, 1991.

Delmonte, B., Petit, J., Andersen, K. K., Basile-Doelsch, I., Maggi, V., and Lipenkov, V. Y.: Dust size evidence for opposite regional atmospheric circulation changes over east Antarctica during the last climatic transition, Clim. Dynam., 23, 427–438, 2004.

Draine, B. T. and Flatau, P. J.: Discrete-dipole approximation for scattering calculations, JOSA A, 11, 1491–1499, 1994.

Grams, G., Blifford Jr, I. H., Gillette, D., and Russell, P.: Complex index of refraction of airborne soil particles, J. Appl. Meteorol., 13, 459–471, 1974.

Hansson, M. E.: The Renland ice core. A Northern Hemisphere record of aerosol composition over 120,000 years, Tellus B, 46, 390–418, 1994.

Jeffery, G. B.: The motion of ellipsoidal particles immersed in a viscous fluid, P. R. Soc. London A, 715, 161–179, 1922.

Kaufmann, P. R., Federer, U., Hutterli, M. A., Bigler, M., Schüpbach, S., Ruth, U., Schmitt, J., and Stocker, T. F.: An improved continuous flow analysis system for high-resolution field measurements on ice cores, Environ. Sci. Technol., 42, 8044–8050, 2008.

Knippertz, P. and Stuut, J.-B. W.: On Composition, Morphology, and Size Distribution of Airborn Mineral Dust, in: Mineral Dust, Springer, 15–50, 2014.

Koffman, B. G., Kreutz, K. J., Breton, D. J., Kane, E. J., Winski, D. A., Birkel, S. D., Kurbatov, A. V., and Handley, M. J.: Centennial-scale variability of the Southern Hemisphere westerly wind belt in the eastern Pacific over the past two millennia, Clim. Past, 10, 1125–1144, https://doi.org/10.5194/cp-10-1125-2014, 2014.

Lambert, F., Delmonte, B., Petit, J. R., Bigler, M., Kaufmann, P. R., Hutterli, M. A., Stocker, T. F., Ruth, U., Steffensen, J. P., and Maggi, V.: Dust-climate couplings over the past 800,000 years from the EPICA Dome C ice core, Nature, 452, 616–619, 2008.

Lambert, F., Bigler, M., Steffensen, J. P., Hutterli, M., and Fischer, H.: Centennial mineral dust variability in high-resolution ice core data from Dome C, Antarctica, Clim. Past, 8, 609–623, https://doi.org/10.5194/cp-8-609-2012, 2012.

Lambert, F., Tagliabue, A., Shaffer, G., Lamy, F., Winckler, G., Farias, L., Gallardo, L., and Pol-Holz, D.: Dust fluxes and iron fertilization in Holocene and Last Glacial Maximum climates, Geophys. Res. Lett., 42, 6014–6023, 2015.

Mahowald, N., Kohfeld, K., Hansson, M., Balkanski, Y., Harrison, S. P., Prentice, I. C., Schulz, M., and Rodhe, H.: Dust sources and deposition during the last glacial maximum and current climate: A comparison of model results with paleodata from ice cores and marine sediments, J. Geophys. Res.-Atmos., 104, 15895–15916, 1999.

Potenza, M. A. C., Albani, S., Delmonte, B., Villa, S., Sanvito, T., Paroli, B., Pullia, A., Baccolo, G., Mahowald, N., and Maggi, V.: Shape and size constraints on dust optical properties from the Dome C ice core, Antarctica, Sci. Rep., 6, 28162, https://doi.org/10.1038/srep28162, 2016.

Röthlisberger, R., Bigler, M., Hutterli, M., Sommer, S., Stauffer, B., Junghans, H. G., and Wagenbach, D.: Technique for continuous high-resolution analysis of trace substances in firn and ice cores, Environ. Sci. Technol., 34, 338–342, 2000.

Royer, A., De Angelis, M., and Petit, J.: A 30000 year record of physical and optical properties of microparticles from an East Antarctic ice core and implications for paleoclimate reconstruction models, Climatic Change, 5, 381–412, 1983.

Ruth, U.: Concentration and size distribution of microparticles in the NGRIP ice core (Central Greenland) during the last glacial period, Ph.D. thesis, University of Bremen, 2002.

Ruth, U., Wagenbach, D., Steffensen, J. P., and Bigler, M.: Continuous record of microparticle concentration and size distribution in the central Greenland NGRIP ice core during the last glacial period, J. Geophys. Res.-Atmos., 108, 1-1–1-12, 2003.

Ruth, U., Barbante, C., Bigler, M., Delmonte, B., Fischer, H., Gabrielli, P., Gaspari, V., Kaufmann, P., Lambert, F., Maggi, V., Marino, F., Petit, J.-R., Udisti, R.,, Wagenbach, Wegner, A., and Wolff, E. W.: Proxies and measurement techniques for mineral dust in Antarctic ice cores, Environ. Sci. Technol., 42, 5675–5681, 2008.

Shettle, E. P. and Fenn, R. W.: Models for the aerosols of the lower atmosphere and the effects of humidity variations on their optical properties, Tech. Rep., Air Force Geophysics Laboratory Hanscom Air Force Base, Mass., USA, 1979.

Sokolik, I., Andronova, A., and Johnson, T. C.: Complex refractive index of atmospheric dust aerosols, Atmos. Environ. Pt. A, 27, 2495–2502, 1993.

Steffensen, J. P.: The size distribution of microparticles from selected segments of the Greenland Ice Core Project ice core representing different climatic periods, J. Geophys. Res.-Ocean., 102, 26755–26763, 1997.

van de Hulst, H. C.: Light scattering by small particles, Courier Corporation, 1957.

Villa, S., Sanvito, T., Paroli, B., Pullia, A., Delmonte, B., and Potenza, M. A. C.: Measuring shape and size of micrometric particles from the analysis of the forward scattered field, J. Appl. Phys., 119, 224901, https://doi.org/10.1063/1.4953332, 2016.

Yurkin, M. A. and Hoekstra, A. G.: The discrete-dipole-approximation code ADDA: capabilities and known limitations, Journal of Quantitative Spectroscopy and Radiative Transfer, 112, 2234–2247, 2011.